

1 **Growth increments of coralline red alga *Clathromorphum compactum* capture**
2 **sea-ice variability links to Atlantic Multidecadal and Arctic Oscillations (1805 – 2015)**
3

4 **N. Leclerc^{1,2}, J. Halfar¹, S. Hetzinger³, A. Tsay⁴, and G. W. K. Moore¹**

5 ¹Chemical and Physical Sciences Department, University of Toronto Mississauga, 3359
6 Mississauga Road N., Ontario, L5L 1C6, Canada

7 ²Department of Archaeology, Memorial University of Newfoundland, 210 Prince Philip Dr.,
8 Newfoundland & Labrador, A1C 5S7

9 ³Christian-Albrechts-Universität zu Kiel, Institut für Geowissenschaften, Ludewig-Meyn-Str.
10 10, 24118 Kiel, Germany

11 ⁴Department of Earth Sciences, University of Geneva, Rue des Maraichers 13, 1205, Geneva,
12 Switzerland

13 Corresponding author: Natasha Leclerc (natasha.leclerc@mail.utoronto.ca)

14 **Key Points:**

- 15 • Algal growth increments correlate most strongly with Atlantic Multidecadal Oscillation
16 (AMO) but also with Arctic Oscillation (AO) trends.
- 17 • The algal record points to sea-ice reduction leading a positive AMO phase in the early to
18 mid-1800s and Early Twentieth Century Warming.
- 19 • The algal proxy record from Lancaster Sound captures +AO-related sea-ice export into
20 the Canadian Arctic Archipelago.
21

22 Abstract

23 The Atlantic Multidecadal Oscillation (AMO), Arctic Oscillation (AO), and related North
24 Atlantic Oscillation (NAO) have been linked to multidecadal, decadal, and/or interannual sea-ice
25 variability in the arctic, but their relative influences are still under evaluation. While instrumental
26 AMO and reliable AO records are available since the mid-1800s and 1958, respectively, satellite
27 sea-ice concentration datasets start only in 1979, limiting the shared timespan to study their
28 interplay. Growth increments of the coralline algae, *Clathromorphum compactum*, can provide
29 sea-ice proxy information for years prior to 1979. We present a seasonal 210-year algal record
30 from Lancaster Sound in the Canadian Arctic Archipelago capturing low frequency AMO
31 variability and high frequency interannual AO/NAO prior to 2000. We suggest that sea-ice
32 variability here is strongly coupled to these large-scale climate processes, and that sea-ice cover
33 was greater and the AO more negative in the early and late 19th century compared to the 20th.

34 Plain Language Summary

35 Arctic sea-ice variability is dually related to air/ocean temperatures and dynamic forces (wind
36 patterns and ocean currents). While long-term basin-averaged temperature trends (i.e., Atlantic
37 Multidecadal Oscillation) tend to influence variability over decades, cyclical wind patterns (e.g.,
38 Arctic Oscillation), may instead influence it seasonally and interannually. When the Atlantic
39 Multidecadal and/or Arctic Oscillation (AMO/AO) are in a positive phase, warmer air and winds
40 tend to export sea-ice out of the Arctic, and vice-versa during negative phases. Unfortunately, the
41 span of the satellite sea-ice cover record is too short to study long-term sea-ice variability driven
42 by these patterns. Therefore, proxy records are required to fill this gap. The tree-ring-like growth
43 bands of an Arctic coralline red algae have produced multi-centennial proxy sea-ice cover
44 records. We present a 210-year algal sea-ice proxy record, showing a relationship with
45 instrumental AMO (1861 – present) and AO records (1958 – 2000). It also suggests that the AO
46 was more negative and sea-ice cover was greater during the 19th century in comparison to the
47 20th century. Due to sea-ice's role in global climate at different timescales, this record can be
48 utilized to tweak climate models or constrain the relative influence of internal forcing on sea-ice
49 behaviour.

50

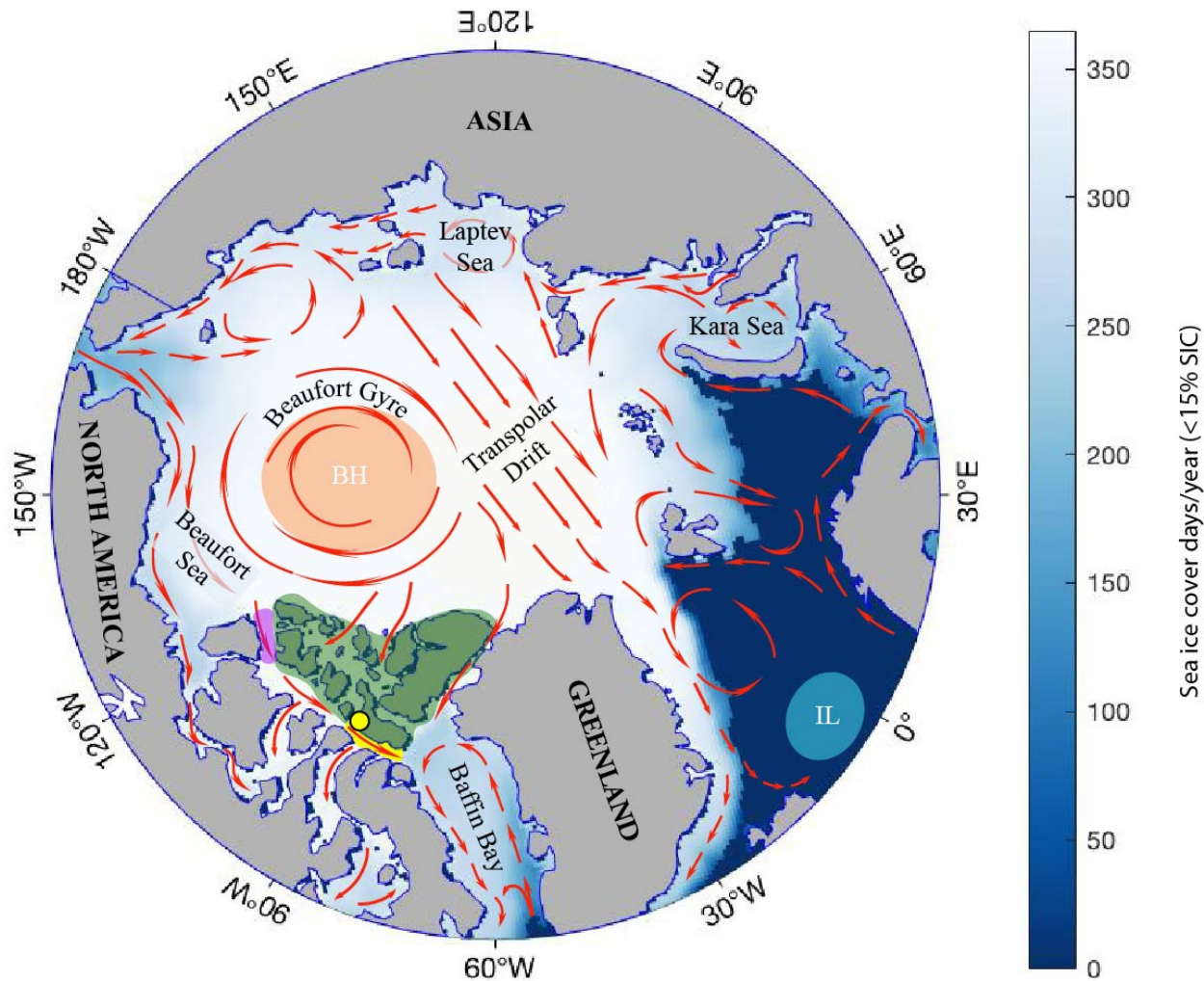
51 **1 Introduction**

52 Since the late 1970s, satellite imagery has made it possible to observe the rapid decline of arctic
 53 sea-ice, especially noticeable in the summer (perennial extent: (Nghiem et al., 2006); thickness:
 54 (Kwok & Rothrock, 2009); duration (Galley et al., 2016)). Warming caused by greenhouse gases
 55 (GHG) and other aerosol emissions, such as black carbon, are often cited as significant
 56 anthropogenic contributors to sea-ice decline (GHG: (Zhang & Walsh, 2006); aerosols Willis et
 57 al., 2018); black carbon: (Kim et al., 2005; Shindell & Faluvegi, 2009). Feedback mechanisms
 58 have also contributed to the warming trend, such as the ice-albedo feedback (Meier et al., 2014;
 59 Perovich et al., 2007), and the increasingly ice-free ocean surface promoting higher spring cloud
 60 coverage, trapping longwave radiation causing more ice melt (Francis & Hunter, 2006). Further,
 61 the respective natural variability of basin-wide oceanic temperatures and large-scale atmospheric
 62 patterns like the Atlantic Multidecadal Oscillation (AMO; a.k.a. Atlantic Multidecadal
 63 Variability), and the Arctic Oscillation (AO; a.k.a., Northern Annular Mode), and the related
 64 North Atlantic Oscillation (NAO), have also been shown to influence sea-ice variability (Divine
 65 & Dick, 2006; Miles et al., 2014; Rigor et al., 2002) and the recently observed decline in sea-ice
 66 conditions (Gillett et al., 2002; Rigor & Wallace, 2004; Rigor et al., 2002; Thompson & Wallace,
 67 1998). Evidently, many factors control arctic sea-ice variability, yet the relative roles that natural
 68 and anthropogenic forces play are still uncertain (Delworth et al., 2016). Further, reliable
 69 satellite sea-ice records are only available since the late 1970s and AO records prior to 1958 have
 70 many associated inconsistencies, challenging the ability to resolve how long-term natural climate
 71 patterns drive sea-ice variability.

72
 73 In the absence of long instrumental records, tree-ring- or coral-based proxy records (Gray et al.,
 74 2004; Saenger et al., 2009), multi-proxy (terrestrial, ice core, lacustrine or coral archives: Mann
 75 et al., 1995) and modelled (Delworth & Mann, 2000) AMO records have attempted to clarify the
 76 periodicity of the AMO. Other studies have used historical and proxy records to study the
 77 interplay between AMO and sea-ice (Divine & Dick, 2006; Frankcombe et al., 2010; Macias-
 78 Fauria et al., 2010). Similar work has been accomplished with AO reconstructions which have
 79 also used the previously discussed archives (D'Arrigo et al., 2003; Rimbu et al., 2001; Rimbu et
 80 al., 2003; Sicre et al., 2014; Young et al., 2012), and deep-sea sediment cores (Darby, Ortiz,
 81 Grosch, & Lund, 2012). Important limitations of sediment cores are that they typically provide
 82 lower-temporal resolution records than tree-ring, coral, ice-core, and lake varve records, while
 83 the latter archives have been unable to directly capture oceanic or regional variability north of
 84 the tree line.

85
 86 Alternatively, the annually-banded skeleton of the calcified coralline red algae species
 87 *Clathromorphum compactum* has been used to build direct oceanic proxy timeseries for arctic
 88 sea-ice changes and other environmental parameters (sea-ice: Halfar et al., 2013; Hetzinger et al.,
 89 2019; Leclerc et al., 2021, 2022; temperature variability: (Gamboa et al., 2010; Halfar et al.,
 90 2011; Halfar et al., 2008; Hetzinger et al., 2018; Hou et al., 2018; Williams et al., 2018, 2019);
 91 Suess effect: Hou et al., 2018; productivity: (Chan et al., 2017); runoff: (Hetzinger et al., 2021).
 92 This alga has a multi-century lifespan and inhabits shallow (typically <20 m depth) benthic
 93 niches with rocky substrate (Adey, 1966). *C. compactum* can archive variability of summer sea-
 94 ice cover since annual algal growth increment widths are heavily influenced by summer sunlight
 95 access for photosynthesis, which is diminished by overlying sea-ice cover (Williams et al.,
 96 2018). To date, several coralline-algal-sea-ice-proxy (CASIP) records have been produced from

97 *C. compactum* samples collected in the Arctic (Halfar et al., 2013; Hetzinger et al., 2019; Leclerc
 98 et al., 2022). In this study, we show that *C. compactum* growth increment records from Lancaster
 99 Sound in the Canadian Arctic Archipelago indicate a long-term relationship between sea-ice
 100 variability and summer AMO, AO and NAO indices.
 101

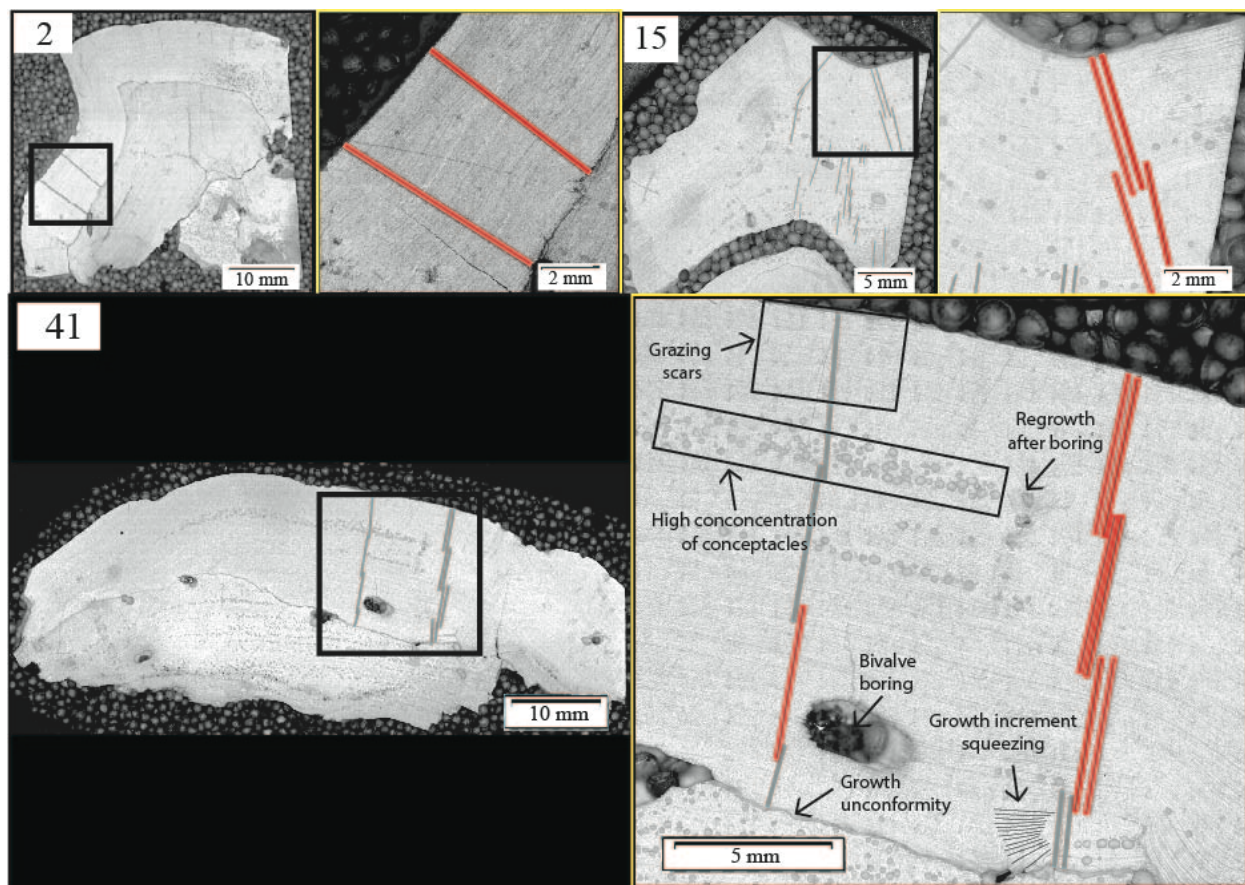


102 **Figure 1.** Representation of negative phase of Arctic Oscillation (AO) in the Arctic Ocean.
 103 Beaufort High (BH; orange); Icelandic Low (IL; light blue); Queen Elizabeth Islands (QEI:
 104 green); M'Clure Strait (purple); Beechey Island algal collection site (yellow dot); Lancaster
 105 Sound (yellow region). Negative AO phases promote a clockwise circulation of the Beaufort
 106 Gyre and are marked by a stronger BH sea level pressure that promotes a counter-clockwise gyre
 107 circulation and ice convergence. The opposite holds true for positive phases. Ocean circulation
 108 shown as red arrows (based on Fig. 3.29 in AMAP, 1998) and length of the ice-on season as
 109 white to dark blue gradient (1979-2015 mean days with >15% SIC: sourced from NSIDC (Meier
 110 et al., 2017)).
 111

112 2 Algal Data Preparation & Analysis Methods

113 Individual *Clathromorphum compactum* buildups were collected at 18-20 metre depths near
 114 Beechey Island, northwestern Lancaster Sound, Nunavut, Canada, via SCUBA in 2016
 115 (74°42'54.46"N, 91°47'29.35"W; Fig. 1). Crusts were prepared into thick sections with an Isomet
 116 Precision Saw, ground and polished with a Struers Labopol polishing disk in 9 μm , 3 μm and 1
 117 μm steps, with ultrasonic bath immersion between steps. Thick sections were then imaged with
 118 an Olympus VS-BX reflected light microscope paired to an automated stage. Images were
 119 stitched together with Geo.TS software and the 3 highest quality specimens (IDs: 2, 15 and 41)
 120 were selected for geochemical analysis (Fig. 2).

121



122

123

124 **Figure 2.** Overview (left) and magnified (right) images of *C. compactum* crusts from Beechey
 125 Island, Lancaster Sound. Laser ablation paths used along axis of growth indicated in red. Sample
 126 IDs shown in upper left corner, respectively.

127

128 Geochemical data were obtained at the University of Toronto's Earth Science Center with a
 129 NWR 193 UC laser ablation inductively coupled mass spectrometry (LA-ICP-MS) system linked
 130 to an Agilent 7900 quadrupole mass spectrometer. Line scans were ablated at a speed of 5
 131 $\mu\text{m}/\text{second}$ along the growth axis, using an aperture size of $10 \times 70 \mu\text{m}$, and a 10 Hz laser pulse
 132 rate (*see details in Hetzinger et al., 2011*). By comparing growth increments visible on
 133 microscope images with the widths of annual Mg/Ca cycles calculated from LA-ICP-MS data,
 134 age models and growth increment width timeseries were built and crossdated between 2 transects

135 for intra-sample replicability and between 3 samples to ensure adequate inter-specimen
136 coherence (for detailed procedures see [Leclerc et al., 2022](#)). Prior to 1880, only sample 41 (3
137 crossdated transects), which provided the longest continuous chronology, was used to extend the
138 record back to 1805. All data was normalized and averaged across crossdated measurements to
139 form a master chronology.

140 **3 Instrumental Data & Statistics**

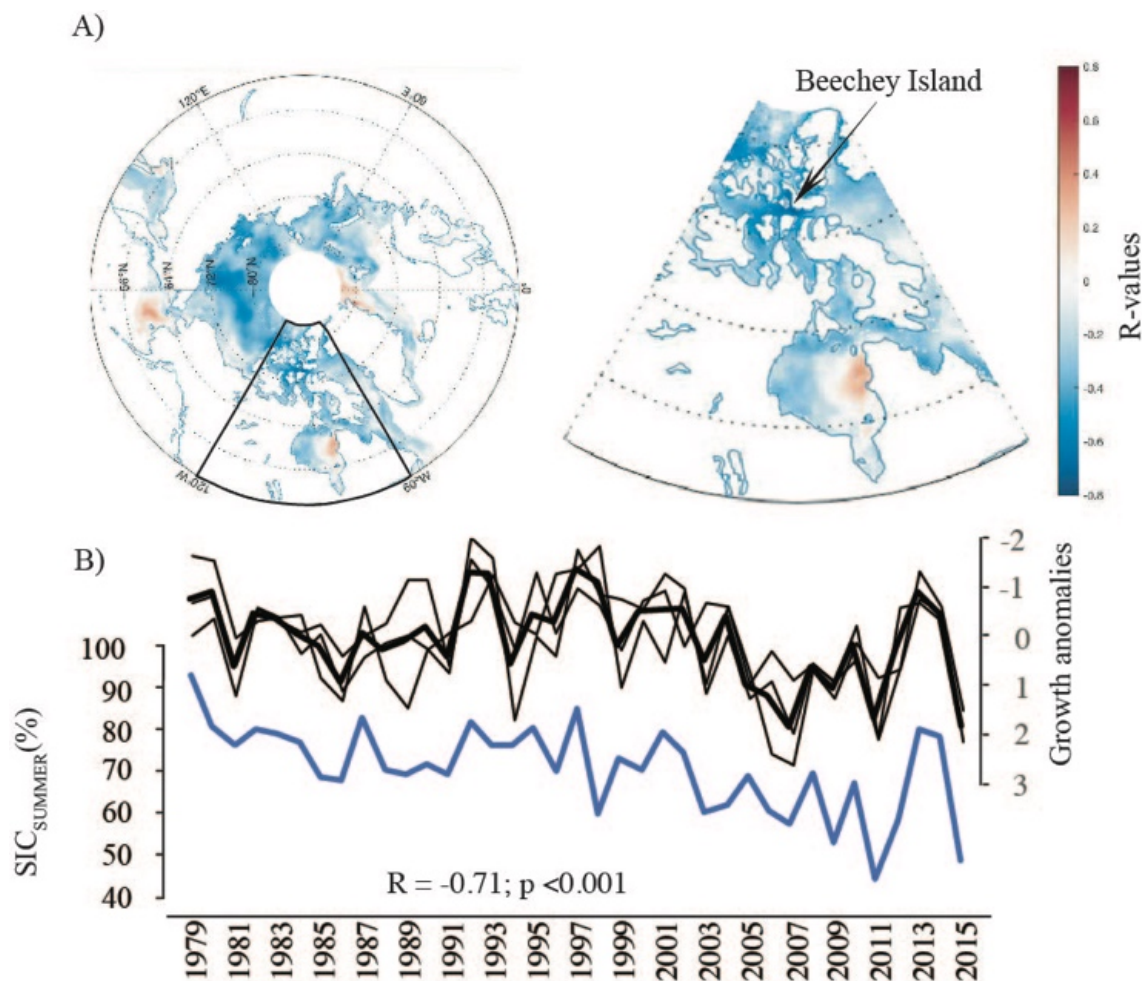
141 Correlation analysis (linear regression) was used to determine the relationship between the algal
142 record and instrumental indices. Monthly AO index values based on instrumental sea level
143 pressure (SLP: Poleward of 20°N calculated by projecting the AO pattern on SLP anomalies)
144 computed through the National Centers for Environmental Prediction–National Center for
145 Atmospheric Research (NCEP/NCAR) reanalysis ([Wallace & Thompson, 2000](#)). Monthly
146 Hurrell North Atlantic Oscillation (NAO) index values are based on principal component
147 analysis of SLP over the Atlantic. While the instrumental AO index goes as far back as 1899,
148 early data issues include different SLP sources for different time periods, with discontinuities
149 identified between data source transitions ([Trenberth & Paolino, 1980](#)). Therefore, only later
150 instrumental AO index values (1958–2015) were used in this study due to confidence issues with
151 early data points. Further, the NAO record was shortened to match the length of the AO record
152 for even comparison to the algal record in [Table 1](#). The correlation between the CASIP record
153 and the full length NAO record is reported and plotted in [Figure 4](#). Monthly AMO index values
154 are the 10-year running mean values smoothed from the Kaplan SST V2 timeseries. Seasonal
155 means were calculated by averaging summer months (May–Oct). Spatial correlation analysis and
156 linear regression to monthly NSIDC sea-ice concentration dataset see procedure in ([Leclerc et
157 al., 2021](#)) was computed using Matlab and `m_map` mapping toolbox. The software `kSpectra` is an
158 implementation of techniques described in [Ghil et al. \(2002\)](#) and was used to run multi-taper and
159 singular spectral analyses (SSA) on instrumental and proxy datasets to determine if the algal
160 record shared AO, NAO and AMO frequency signatures.

161 **4 Results & Discussion**

162 Since higher sea-ice cover, in typically colder years, limits growth, we expected a negative
163 correlation between regional sea-ice cover and annual growth, and positive correlations with AO,
164 NAO, and AMO. Accordingly, spatial correlation analysis shows strongly significant negative
165 correlations ($p < 0.001$) between Beechey Island growth increment chronology and regional
166 satellite sea-ice concentrations ([Fig. 3](#)). Highly significant spatial relationships also centered
167 along the northern coast of the Canadian Arctic Archipelago, the Beaufort Sea and the Laptev
168 Sea ([Fig. 3a](#)). At a more localized scale, the algal growth increment timeseries correlates
169 significantly ($R = -0.71$; $p < 0.001$) with satellite sea-ice concentrations ([Leclerc et al., 2022](#)) ([Fig.
170 3b](#)). The confirmation of the local sea-ice–algal growth relationship suggests that if AMO, AO or
171 NAO and sea-ice are related in Lancaster Sound, the algal timeseries should record their signal.
172 Indeed, correlation analysis demonstrated that the master Beechey Island chronology
173 significantly ($p < 0.001$) captured the decadal-smoothed AMO index ([Tab. 1](#)). The AO was also
174 significantly correlated at annual ($p < 0.01$) and decadal ($p < 0.05$) resolutions, and the NAO
175 correlation was markedly strong at a decadal resolution ($p < 0.001$), however only until 2000.
176

177 The lack of correlation between AO and sea-ice cover in recent decades has previously been
178 documented ([Feldstein, 2002](#); [Overland & Wang, 2005](#); [Overland & Wang, 2010](#); [Stroeve et al.,](#)

179 2011) and this coralline algal record supports it as well. Its manifestation in the Canadian Arctic
 180 Archipelago (CAA) may also be related to recent shifts in the duration of ice bridges, landfast ice
 181 between landmasses which form in winter and block sea-ice export until summer collapse. When
 182 ice bridges at M'Clure Strait or the Queen Elizabeth Islands (QEI) (Fig. 1) collapse, sea-ice from
 183 the Arctic Ocean is free to be imported into the CAA, especially during positive AO phases
 184 (Howell et al., 2013). Contrary to the +AO-stimulated ice breakup/export acceleration, +AO-
 185 stimulated sea-ice import after ice bridge collapse may limit algal light access and mute the AO
 186 signal. In fact, since 2005 there has been an increase of ice inflow into the CAA through the
 187 Queen Elizabeth Islands, which tends to flow south towards Lancaster Sound (Howell et al.,
 188 2013). Other data from the Nares Strait suggest that ice volume export through the Strait has
 189 increased recently in comparison to the 1997-2009 mean, linked to the trend of shorter duration
 190 of ice bridges (Moore et al., 2021). This may be responsible for the masked AO signal in the
 191 Beechey Island CASIP record since the turn of the millennium (Supplementary Figure 1; Tab. 1).
 192



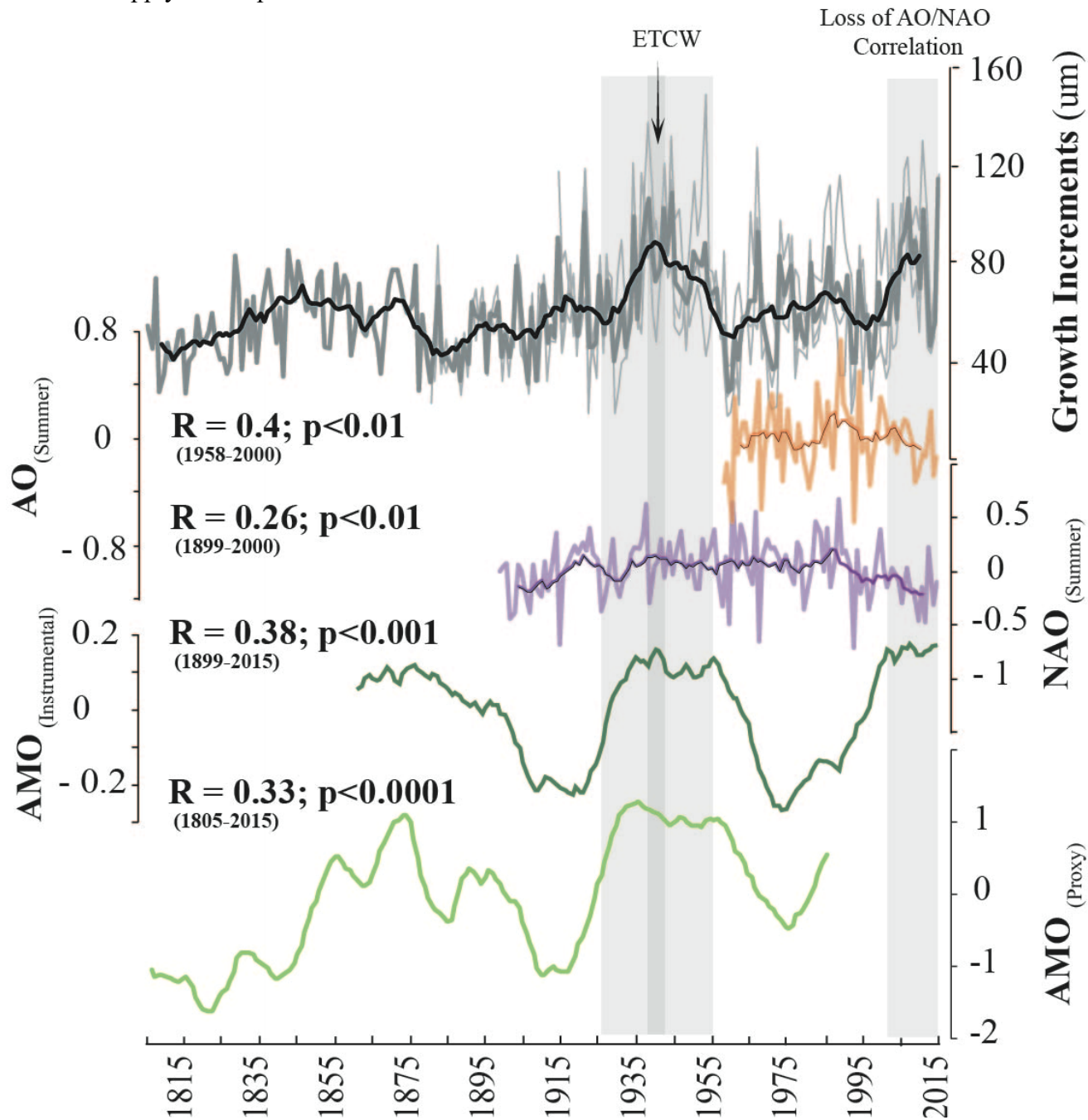
193
 194 **Figure 3.** A) Spatial correlation analysis between gridded Arctic SIC and Beechey Island growth
 195 increment chronology. Right plot shows Beechey Island region enlarged. B) Plotted algal
 196 growth increment timeseries (black: anomalies = (annual value – average) / standard deviation)
 197 and NSIDC sea-ice concentrations (blue: 75 km² around Beechey Island site) (see Leclerc et al.,

198 2022 for original figure of subplot B). Note that growth anomalies are plotted inversely. R-value
199 indicates strength of correlation.

200
201 Periods with larger growth increments coincide with a strongly positive AMO period and the
202 Early Twentieth Century Warming (ETCW: 1920s-1950s) period (Fig. 4). The ETCW has been
203 shown to be associated with sea-ice retreat in the Barents Sea caused by stronger westerly winds
204 between Spitsbergen and Norway (Bengtsson et al., 2004), and has also been recorded by *C.*
205 *compactum* Ba/Ca and growth-Mg/Ca anomaly timeseries from Spitsbergen (Hetzinger et al.,
206 2021, 2019). Day et al. (2012) suggested the recent positive phase of AMO could explain 5-30%
207 of satellite summer sea-ice loss and Miles et al. (2014) suggested AMO was a major driver of
208 sea-ice variability from the past 800 years to the 1990s. Similarly, our data showed that the AMO
209 and ETCW affected ice decline in Lancaster Sound in the mid-20th century. Multi-taper spectral
210 analysis results showed multidecadal variability in the algal chronology (significant at 99% level,
211 60-77-year signal, CASIP: 1805–2015; Supplementary Figure S1), comparable to the posited
212 periodicity of AMO (60–80 years) (Kerr, 2000; Schlesinger & Ramankutty, 1994). Significant
213 (95% level) interannual signals (at 2 and 3 years) were also found, closely matching AO
214 signatures (Supplementary Figure S1) previously shown to affect sea-ice circulation in the Baltic
215 Sea (Jevrejeva et al., 2003). However, the CASIP multi-taper results did not capture AO's
216 decadal variability as reported elsewhere (Ramos da Silva & Avissar, 2005). However, singular
217 spectrum analysis (SSA) of the shortened CASIP record (1960-2000) identified significant
218 variability at 7.6–10.3 years responsible for more than 60% of variance (Supplementary Figure
219 S1). In the AO_{SUMMER} record (1960-2000), most of the variability is interannual (2.5-5.1 years;
220 details in Supplementary Text S1), a decadal signal (10.6-year) is explaining only 16.9% of total
221 variance. In summary, multi-taper and SSA did not fully identify the 8 – 10-year AO signals
222 previously identified through wavelet power spectrum analysis (Ramos da Silva & Avissar,
223 2005). This further suggests that the shared variability at the approximately 2–3-year periodicity
224 level is what the sea-ice-AO and sea-ice-CASIP relationships are recording in the CAA.

225
226 The part of the algal record that extends earlier than the instrumental NAO record (i.e., prior to
227 1899), suggests colder and heavier ice conditions in the 19th century in comparison to the 20th
228 century similar to the findings of indirect (temperature) sea-ice proxy tree ring records (D'Arrigo
229 et al., 2003; Young et al., 2012). The algal chronology also suggests a period of less ice in the
230 mid-1800s possibly due to more positive AO/NAO or AMO, or both (Fig. 4). While, many have
231 suggested that the Little Ice Age and colder conditions persisted until the late 1800s, this slightly
232 warmer period in the mid-1800s is supported by multiple Arctic proxy records that find episodic
233 warming at this time (Jennings & Weiner, 1996; Massé et al., 2008: records synthesized in Miles
234 et al., 2020). This warming period is also corroborated by ice cap stratigraphy from nearby
235 Devon Island, Greenland ice sheets and marine cores from the Labrador Sea, which suggested
236 early warming in 1860s and a more intense warming trend beginning around 1890 (Keigwin et
237 al., 2003; Koerner, 1977; Trusel et al., 2018). The mid-1800s mild warming period found in our
238 record predates those found in other AMO proxy records from terrestrial archives (e.g., Gray et
239 al., 2004), which shows a later warming period later in the 1800s, and cooler 1830s-1840s (Fig.
240 4). While, some suggest some uncertainty in terrestrial AMO records (e.g., Miles et al., 2020), it
241 is notable that sea-ice and NAO trends have been shown to lead AMO variability in some
242 regions, and that the timing in AMO peaks and troughs are regionally variable (Alexander et al.,

243 2014; Peterson et al., 2015). As the NAO and AO are highly correlated (Rigor et al., 2002), this
 244 could also apply to AO precursors to AMO.



245
 246
 247 **Figure 4.** Relationship between crossdated Beechey Island growth increment (i.e., CASIP)
 248 detrended chronology and detrended AO (orange), NAO (purple) and AMO (dark green) climate
 249 indices for summer months (May-October). Individual algal samples (light grey); average of all
 250 algal samples (dark grey); 10-yr running mean of average growth, AO and NAO (black, dark
 251 orange, and dark purple lines, respectively). Tree ring-based proxy AMO timeseries (light green)
 252 from Gray et al. (2004). AMO is 10-year averaged index (no 10-yr running mean). Early

253 Twentieth Century Warming (ETCW: 1920-1960) and loss of correlation in 2000s periods (grey
 254 bars), and major El Niño event (arrow: 1939-1942).

255
 256 Algal-sea-ice-proxy (CASIP) records are indicators of a combination of sea-ice variables
 257 affecting light penetration to the benthos: present/absent ice cover (related to melt/freeze up and
 258 wind and current dynamics), seasonal duration of cover, thickness and snow cover. Together, the
 259 AMO, AO, and NAO have the capacity of affecting all these variables. [Samelson et al. \(2006\)](#)
 260 suggested that the formation of land-fast ice in the CAA is controlled by both winds and air
 261 temperature, both are parameters influenced by these large atmospheric and ocean temperature
 262 patterns. Furthermore, [Peterson et al. \(2012\)](#) found that monthly longshore wind anomalies in the
 263 Beaufort Sea, which are heavily influenced by AO, stimulated 43% of Lancaster Sound’s volume
 264 transport anomaly variance. This is supported by the significant relationship between the
 265 Beechey Island CASIP record and gridded sea-ice concentrations on the exterior CAA coast
 266 bordering the Beaufort Sea ([Fig. 2a](#)). The linked variability and coupling of the AO/NAO and
 267 AMO are posited to stem in part from interannual and long-term sea-ice cover trends and/or
 268 stimulation of Atlantic Meridional Overturning Circulation (AMOC) ([Medhaug et al., 2012](#);
 269 [Peterson et al., 2015](#); [Polyakov et al., 2010](#); [Polyakov et al., 2005](#); [Yang et al., 2016](#)). Our results
 270 seem to support the assertion of arctic sea-ice’s important role in AMO variability.

271 **Table 1.** Linear regression (R- and p-values) correlations of Beechey Island algal growth record
 272 to climate indices at seasonal (summer) and decadal (10-year running means of summer values)
 273 resolutions. Highlighted grey boxes are significant positive correlations ($p < 0.5$; darkest shades
 274 indicate $p < 0.01$).

AO (May-Oct: 1958 -)		NAO (May-Oct: 1958 -)		AMO (Annual: 1861 -)
Seasonal	Decadal	Seasonal	Decadal	Decadal
Anomalies (- 2015)				
0.23 p=0.08	-0.11 p=0.4	0.05 p=0.7	-0.49 p<0.001	0.31 p= 0.001
Anomalies (- 2000)				
0.41 p<0.01	0.41 p<0.01	0.33 p=0.03	0.53 p<0.001	0.21 p= 0.01
Detrended (- 2015)				
0.17 p=0.2	-0.37 p<0.01	0.08 p=0.55	-0.4 p<0.01	0.39 p<0.001
Detrended (- 2000)				
0.4 p<0.01	0.31 p<0.05	0.34 p<0.05	0.64 p<0.001	0.38 p<0.001
Note. All negative correlations are considered insignificant.				

275 5 Summary & Conclusion

276 The *C. compactum* growth increment chronology from Beechey Island recorded: 1) lower sea-ice
 277 cover during the 1800s in comparison to the 1900s; 2) slightly lighter sea-ice years in the mid-
 278 1800s; 3) the Earth Twentieth Century Warming period; 4) significant sea-ice response to AMO
 279 throughout the record; 5) significant sea-ice responses to AO/NAO from 1960-2000, and; 6) lack
 280 of sea-ice response to AO/NAO from 2000-2015 possibly due to external factors such as the
 281 greenhouse gas (GHG) effect and ice-albedo feedbacks. The development of longer high-
 282 resolution proxy records such as CASIP timeseries is critical to understanding the role of
 283 cryospheric-atmospheric feedbacks in the many intertwined components in the global climate
 284 system (Gao et al., 2015). The Canadian Arctic Archipelago, which tends to trap multi-year ice
 285 (Howell et al., 2008; Kwok, 2015), makes up a significant part of the *Last Ice Area*, predicted to
 286 be the last arctic region to experience summer ice cover (Moore et al., 2019). As this area will
 287 become increasingly crucial in the coming years, and potentially more hazardous to naval travel
 288 (Howell et al., 2022), *C. compactum* CASIP records can provide important historical and pre-
 289 industrial baselines. While it is reasonably well understood that atmospheric patterns have an
 290 effect on sea-ice extent, the interplay between coastal sea-ice cover and atmospheric patterns,
 291 especially in the CAA is still not well understood. Here we find strong links between internal
 292 variability and sea-ice trends. However, we note that these links are muted in recent decades
 293 (especially after 2000) due to anthropogenic forcing and possibly enhancement of ice penetration
 294 through QEI gates in the Canadian Arctic Archipelago (Howell et al., 2023).

295 Acknowledgments

296 Funding support: NSERC Discovery (1303409; J.H.); NSERC CGS-D (CGSD3-518838 – 2018;
 297 N.L.); DFG (Grant HE 6251/10-1 to S. H.); NSERC to G.W.K.M. We also thank the Earth
 298 Sciences Department of the University of Toronto, the Earth Sciences Lab at UTM, and Dr. Max
 299 Friesen and Dr. Sarah Finkelstein for feedback, insights and questions that helped in the
 300 development of this manuscript.

301 Open Research

302 This article contains original data (algal chronologies 1805-1870) and previously published data
 303 (algal chronologies 1871-2015) which is available in (Leclerc et al., 2022). Original data extend
 304 the previously published record. All coralline red algae data sets have been submitted to the
 305 NOAA National Centers for Environmental Information Paleoclimatology Data Repository
 306 (*awaiting official doi*). Primary data sets for this research are also included in figures and
 307 Supporting Information S1 files. Environmental data sets include: The monthly AO Index values
 308 were extracted from KMNI Climate Explorer (based on Trenberth & Paolino, 1980). Monthly
 309 Hurrell North Atlantic Oscillation (NAO) index values were extracted from NCAR Climate Data
 310 Guide (<https://climatedataguide.ucar.edu/>). Monthly AMO 10-year running mean values
 311 smoothed from the Kaplan SST V2 were extracted from NOAA PSL1
 312 (<http://www.psl.noaa.gov/data/timeseries/AMO/>). Spatial correlation analysis and linear
 313 regression to monthly NSIDC sea-ice concentration dataset (Version 3:
 314 <https://nsidc.org/data/g02202>; Peng et al., 2013; Meier et al., 2017; see procedure in (Leclerc et
 315 al., 2021) was computed using Matlab and `m_map` mapping toolbox. The software `kSpectra`
 316 described in Ghil et al. (2002) was used to run multi-taper and singular spectral analyses.

317

318 **References**

- 319 Adey, W. H. (1966). Distribution of saxicolous crustose corallines in the northwestern North
 320 Atlantic. *Journal of Phycology*, 2(2), 49–54. [https://doi.org/10.1111/J.1529-](https://doi.org/10.1111/J.1529-8817.1966.TB04593.X)
 321 [8817.1966.TB04593.X](https://doi.org/10.1111/J.1529-8817.1966.TB04593.X)
- 322 Alexander, M. A., Halimeda Kilbourne, K., & Nye, J. A. (2014). Climate variability during
 323 warm and cold phases of the Atlantic Multidecadal Oscillation (AMO) 1871–2008. *Journal*
 324 *of Marine Systems*, 133, 14–26.
 325 [https://doi.org/https://doi.org/10.1016/j.jmarsys.2013.07.017](https://doi.org/10.1016/j.jmarsys.2013.07.017)
- 326 AMAP. (1998). *AMAP Assessment Report: Arctic Pollution Issues*. Oslo, Norway. Retrieved
 327 from [https://www.amap.no/documents/doc/amap-assessment-report-arctic-pollution-](https://www.amap.no/documents/doc/amap-assessment-report-arctic-pollution-issues/68)
 328 [issues/68](https://www.amap.no/documents/doc/amap-assessment-report-arctic-pollution-issues/68)
- 329 Bengtsson, L., Semenov, V. A., & Johannessen, O. M. (2004). The Early Twentieth-Century
 330 Warming in the Arctic—A Possible Mechanism. *Journal of Climate*, 17(20), 4045–4057.
 331 [https://doi.org/10.1175/1520-0442\(2004\)017<4045:TETWIT>2.0.CO;2](https://doi.org/10.1175/1520-0442(2004)017<4045:TETWIT>2.0.CO;2)
- 332 Chan, P., Halfar, J., Adey, W., Hetzinger, S., Zack, T., Moore, G. W. K., ... Hou, A. (2017).
 333 Multicentennial record of Labrador Sea primary productivity and sea-ice variability
 334 archived in coralline algal barium. *Nature Communications*, 8(1), 1–10.
 335 <https://doi.org/10.1038/ncomms15543>
- 336 D'Arrigo, R. D., Cook, E. R., Mann, M. E., & Jacoby, G. C. (2003). Tree-ring reconstructions of
 337 temperature and sea-level pressure variability associated with the warm-season Arctic
 338 Oscillation since AD 1650. *Geophysical Research Letters*, 30(11), 1549.
 339 <https://doi.org/10.1029/2003GL017250>
- 340 Darby, D. A., Ortiz, J. D., Grosch, C. E., & Lund, S. P. (2012). 1,500-year cycle in the Arctic
 341 Oscillation identified in Holocene Arctic sea-ice drift. *Nature Geoscience*, 5(12), 897–900.
 342 <https://doi.org/10.1038/ngeo1629>
- 343 Day, J. J., Hargreaves, J. C., Annan, J. D., & Abe-Ouchi, A. (2012). Sources of multi-decadal
 344 variability in Arctic sea ice extent. *Environmental Research Letters*, 7(3), 034011.
 345 <https://doi.org/10.1088/1748-9326/7/3/034011>
- 346 Delworth, T L, & Mann, M. E. (2000). Observed and simulated multidecadal variability in the
 347 Northern Hemisphere. *Climate Dynamics*, 16(9), 661–676.
 348 <https://doi.org/10.1007/s003820000075>
- 349 Delworth, Thomas L, Zeng, F., Vecchi, G. A., Yang, X., Zhang, L., & Zhang, R. (2016). The
 350 North Atlantic Oscillation as a driver of rapid climate change in the Northern Hemisphere.
 351 *Nature Geoscience*, 9(7), 509–512. <https://doi.org/10.1038/ngeo2738>
- 352 Divine, D. V., & Dick, C. (2006). Historical variability of sea ice edge position in the Nordic
 353 Seas. *Journal of Geophysical Research*, 111(C1), C01001.
 354 <https://doi.org/10.1029/2004JC002851>
- 355 Feldstein, S. B. (2002). The Recent Trend and Variance Increase of the Annular Mode. *Journal*
 356 *of Climate*, 15(1), 88–94. [https://doi.org/10.1175/1520-](https://doi.org/10.1175/1520-0442(2002)015<0088:TRTAVI>2.0.CO;2)
 357 [0442\(2002\)015<0088:TRTAVI>2.0.CO;2](https://doi.org/10.1175/1520-0442(2002)015<0088:TRTAVI>2.0.CO;2)
- 358 Francis, J. A., & Hunter, E. (2006). New insight into the disappearing Arctic sea ice. *Eos*,
 359 *Transactions American Geophysical Union*, 87(46), 509–511.
 360 <https://doi.org/10.1029/2006EO460001>
- 361 Frankcombe, L. M., von der Heydt, A., & Dijkstra, H. A. (2010). North Atlantic Multidecadal
 362 Climate Variability: An Investigation of Dominant Time Scales and Processes. *Journal of*
 363 *Climate*, 23(13), 3626–3638. <https://doi.org/https://doi.org/10.1175/2010JCLI3471.1>

- 364 Galley, R. J., Babb, D., Ogi, M., Else, B. G. T., Geilfus, N. X., Crabeck, O., ... Rysgaard, S.
 365 (2016). Replacement of multiyear sea ice and changes in the open water season duration in
 366 the Beaufort Sea since 2004. *Journal of Geophysical Research: Oceans*, *121*(3), 1806–
 367 1823. <https://doi.org/10.1002/2015JC011583>
- 368 Gamboa, G., Halfar, J., Hetzinger, S., Adey, W., Zack, T., Kunz, B., & Jacob, D. E. (2010).
 369 Mg/Ca ratios in coralline algae record northwest Atlantic temperature variations and North
 370 Atlantic Oscillation relationships. *Journal of Geophysical Research*, *115*(C12), C12044.
 371 <https://doi.org/10.1029/2010JC006262>
- 372 Gao, Y., Sun, J., Li, F., He, S., Sandven, S., Yan, Q., ... Suo, L. (2015). Arctic sea ice and
 373 Eurasian climate: A review. *Advances in Atmospheric Sciences* *2015* *32*:1, *32*(1), 92–114.
 374 <https://doi.org/10.1007/S00376-014-0009-6>
- 375 Ghil, M., Allen, M. R., Dettinger, M. D., Ide, K., Kondrashov, D., Mann, M. E., ... Yiou, P.
 376 (2002). Advanced spectral methods for climatic time series. *Reviews of Geophysics*, *40*(1),
 377 3–1. <https://doi.org/10.1029/2000RG000092>
- 378 Gillett, N. P., Allen, M. R., McDonald, R. E., Senior, C. A., Shindell, D. T., & Schmidt, G. A.
 379 (2002). How linear is the Arctic Oscillation response to greenhouse gases? *Journal of*
 380 *Geophysical Research: Atmospheres*, *107*(D3), ACL 1-1.
 381 <https://doi.org/10.1029/2001JD000589>
- 382 Gray, S. T., Graumlich, L. J., Betancourt, J. L., & Pederson, G. T. (2004). A tree-ring based
 383 reconstruction of the Atlantic Multidecadal Oscillation since 1567 A.D. *Geophysical*
 384 *Research Letters*, *31*(12). <https://doi.org/10.1029/2004GL019932>
- 385 Halfar, J., Hetzinger, S., Adey, W., Zack, T., Gamboa, G., Kunz, B., ... Jacob, D. E. (2011).
 386 Coralline algal growth-increment widths archive North Atlantic climate variability.
 387 *Palaeogeography, Palaeoclimatology, Palaeoecology*, *302*(1), 71–80.
 388 <https://doi.org/10.1016/j.palaeo.2010.04.009>
- 389 Halfar, Jochen, Adey, W. H., Kronz, A., Hetzinger, S., Edinger, E., & Fitzhugh, W. W. (2013).
 390 Arctic sea-ice decline archived by multicentury annual-resolution record from crustose
 391 coralline algal proxy. *Proceedings of the National Academy of Sciences*, *110*(49), 19737–
 392 19741. <https://doi.org/10.1073/pnas.1313775110>
- 393 Halfar, Jochen, Steneck, R. S., Joachimski, M., Kronz, A., & Wanamaker, A. D. (2008).
 394 Coralline red algae as high-resolution climate recorders. *Geology*, *36*(6), 463–466.
 395 <https://doi.org/10.1130/G24635A.1>
- 396 Hetzinger, S., Halfar, J., Kronz, A., Simon, K., Adey, W. H., & Steneck, R. S. (2018).
 397 Reproducibility of *Clathromorphum compactum* coralline algal Mg/Ca ratios and
 398 comparison to high-resolution sea surface temperature data. *Geochimica et Cosmochimica*
 399 *Acta*, *220*, 96–109.
- 400 Hetzinger, S., Halfar, J., Zack, T., Gamboa, G., Jacob, D. E., Kunz, B. E., ... Steneck, R. S.
 401 (2011). High-resolution analysis of trace elements in crustose coralline algae from the North
 402 Atlantic and North Pacific by laser ablation ICP-MS. *Palaeogeography, Palaeoclimatology,*
 403 *Palaeoecology*, *302*(1), 81–94. <https://doi.org/10.1016/j.palaeo.2010.06.004>
- 404 Hetzinger, Steffen, Halfar, J., Zajacz, Z., Möller, M., & Wisshak, M. (2021). Late twentieth
 405 century increase in northern Spitsbergen (Svalbard) glacier-derived runoff tracked by
 406 coralline algal Ba/Ca ratios. *Climate Dynamics*, *56*(9), 3295–3303.
 407 <https://doi.org/10.1007/s00382-021-05642-x>
- 408 Hetzinger, Steffen, Halfar, J., Zajacz, Z., & Wisshak, M. (2019). Early start of 20th-century
 409 Arctic sea-ice decline recorded in Svalbard coralline algae. *Geology*, *47*(10), 963–967.

- 410 <https://doi.org/10.1130/G46507.1>
- 411 Hou, A., Halfar, J., Adey, W., Wortmann, U. G., Zajacz, Z., Tsay, A., ... Chan, P. (2018). Long-
 412 lived coralline alga records multidecadal variability in Labrador Sea carbon isotopes.
 413 *Chemical Geology*, 526(August 2017). <https://doi.org/10.1016/j.chemgeo.2018.02.026>
- 414 Howell, S E L, Babb, D. G., Landy, J. C., Moore, G. W. K., Montpetit, B., & Brady, M. (2023).
 415 A Comparison of Arctic Ocean Sea Ice Export Between Nares Strait and the Canadian
 416 Arctic Archipelago. *Journal of Geophysical Research: Oceans*, 128(4), e2023JC019687.
 417 <https://doi.org/https://doi.org/10.1029/2023JC019687>
- 418 Howell, Stephen E.L., Tivy, A., Yackel, J. J., & McCourt, S. (2008). Multi-year sea-ice
 419 conditions in the western Canadian Arctic Archipelago region of the Northwest Passage:
 420 1968-2006. *Atmosphere - Ocean*, 46(2), 229–242. <https://doi.org/10.3137/ao.460203>
- 421 Howell, Stephen E.L., Wohlleben, T., Dabboor, M., Derksen, C., Komarov, A., & Pizzolato, L.
 422 (2013). Recent changes in the exchange of sea ice between the Arctic Ocean and the
 423 Canadian Arctic Archipelago. *Journal of Geophysical Research: Oceans*, 118(7), 3595–
 424 3607. <https://doi.org/10.1002/JGRC.20265>
- 425 Howell, Stephen E L, Babb, D. G., Landy, J. C., & Brady, M. (2022). Multi-Year Sea Ice
 426 Conditions in the Northwest Passage: 1968–2020. *Atmosphere-Ocean*, 1–15.
 427 <https://doi.org/10.1080/07055900.2022.2136061>
- 428 Jennings, A. E., & Weiner, N. J. (1996). Environmental change in eastern Greenland during the
 429 last 1300 years: evidence from foraminifera and lithofacies in Nansen Fjord, 68°N. *The*
 430 *Holocene*, 6(2), 179–191. <https://doi.org/10.1177/095968369600600205>
- 431 Jevrejeva, S., Moore, J. C., & Grinsted, A. (2003). Influence of the Arctic Oscillation and El
 432 Niño-Southern Oscillation (ENSO) on ice conditions in the Baltic Sea: The wavelet
 433 approach. *Journal of Geophysical Research: Atmospheres*, 108(D21), 4677.
 434 <https://doi.org/10.1029/2003JD003417>
- 435 Keigwin, L. D., Sachs, J. P., & Rosenthal, Y. (2003). A 1600-year history of the Labrador
 436 Current off Nova Scotia. *Climate Dynamics*, 21(1), 53–62. [https://doi.org/10.1007/S00382-
 437 003-0316-6/FIGURES/6](https://doi.org/10.1007/S00382-003-0316-6/FIGURES/6)
- 438 Kerr, R. A. (2000). A North Atlantic Climate Pacemaker for the Centuries. *Science*, 288(5473),
 439 1984–1986. <https://doi.org/10.1126/SCIENCE.288.5473.1984>
- 440 Kim, Y., Hatsushika, H., Muskett, R. R., & Yamazaki, K. (2005). Possible effect of boreal
 441 wildfire soot on Arctic sea ice and Alaska glaciers. *Atmospheric Environment*, 39(19),
 442 3513–3520. <https://doi.org/10.1016/J.ATMOSENV.2005.02.050>
- 443 Koerner, R. M. (1977). Devon Island Ice Cap: Core Stratigraphy and Paleoclimate. *Science*,
 444 196(4285), 15–18. <https://doi.org/10.1126/SCIENCE.196.4285.15>
- 445 Kwok, R., & Rothrock, D. A. (2009). Decline in Arctic sea ice thickness from submarine and
 446 ICESat records: 1958–2008. *Geophysical Research Letters*, 36(15), 15501.
 447 <https://doi.org/10.1029/2009GL039035>
- 448 Kwok, Ron. (2015). Sea ice convergence along the Arctic coasts of Greenland and the Canadian
 449 Arctic Archipelago: Variability and extremes (1992–2014). *Geophysical Research Letters*,
 450 42(18), 7598–7605. <https://doi.org/10.1002/2015GL065462>
- 451 Leclerc, N., Halfar, J., Hetzinger, S., Chan, P. T. W., Adey, W., Tsay, A., ... Kronz, A. (2021).
 452 Suitability of the Coralline Alga *Clathromorphum compactum* as an Arctic Archive for Past
 453 Sea Ice Cover. *Paleoceanography and Paleoclimatology*, 37(1).
 454 <https://doi.org/10.1029/2021PA004286>
- 455 Leclerc, N., Halfar, J., Porter, T. J., Black, B. A., Hetzinger, S., Zulian, M., & Tsay, A. (2022).

- 456 Utility of Dendrochronology Crossdating Methods in the Development of Arctic Coralline
 457 Red Algae *Clathromorphum compactum* Growth Increment Chronology for Sea Ice Cover
 458 Reconstruction. *Frontiers in Marine Science*, 9, 906.
 459 <https://doi.org/10.3389/fmars.2022.923088>
- 460 Macias-Fauria, M., Grinsted, A., Helama, S., Moore, J., Timonen, M., Martma, T., ... Eronen,
 461 M. (2010). Unprecedented low twentieth century winter sea ice extent in the Western
 462 Nordic Seas since A.D. 1200. *Climate Dynamics*, 34(6), 781–795.
 463 <https://doi.org/10.1007/s00382-009-0610-z>
- 464 Mann, M. E., Park, J., & Bradley, R. S. (1995). Global interdecadal and century-scale climate
 465 oscillations during the past five centuries. *Nature*, 378(6554), 266–270.
 466 <https://doi.org/10.1038/378266a0>
- 467 Massé, G., Rowland, S. J., Sicre, M.-A., Jacob, J., Jansen, E., & Belt, S. T. (2008). Abrupt
 468 climate changes for Iceland during the last millennium: Evidence from high resolution sea
 469 ice reconstructions. *Earth and Planetary Science Letters*, 269(3–4), 565–569.
 470 <https://doi.org/10.1016/J.EPSL.2008.03.017>
- 471 Medhaug, I., Langehaug, H. R., Eldevik, T., Furevik, T., & Bentsen, M. (2012). Mechanisms for
 472 decadal scale variability in a simulated Atlantic meridional overturning circulation. *Climate*
 473 *Dynamics*, 39(1), 77–93. <https://doi.org/10.1007/s00382-011-1124-z>
- 474 Meier, W. N., Fetterer, F., Savoie, M., Mallory, S., Duerr, R., & Stroeve, J. (2017).
 475 *NOAA/NSIDC Climate Data Record of Passive Microwave Sea Ice Concentration*. Boulder,
 476 Colorado: NSIDC: National Snow and Ice Data Center.
 477 <https://doi.org/https://doi.org/10.7265/N59P2ZTG>
- 478 Meier, Walter N., Hovelsrud, G. K., van Oort, B. E. H., Key, J. R., Kovacs, K. M., Michel, C.,
 479 ... Reist, J. D. (2014). Arctic sea ice in transformation: A review of recent observed
 480 changes and impacts on biology and human activity. *Reviews of Geophysics*, 52(3), 185–
 481 217. <https://doi.org/10.1002/2013RG000431>
- 482 Miles, M. W., Andresen, C. S., & Dylmer, C. V. (2020). Evidence for extreme export of Arctic
 483 sea ice leading the abrupt onset of the Little Ice Age. *Science Advances*, 6(38), 4320–4336.
 484 https://doi.org/10.1126/SCIADV.ABA4320/SUPPL_FILE/ABA4320_SM.PDF
- 485 Miles, M. W., Divine, D. V., Furevik, T., Jansen, E., Moros, M., & Ogilvie, A. E. J. (2014). A
 486 signal of persistent Atlantic multidecadal variability in Arctic sea ice. *Geophysical Research*
 487 *Letters*, 41(2), 463–469. <https://doi.org/10.1002/2013GL058084>
- 488 Moore, G. W. K., Howell, S. E. L., Brady, M., Xu, X., & McNeil, K. (2021). Anomalous
 489 collapses of Nares Strait ice arches leads to enhanced export of Arctic sea ice. *Nature*
 490 *Communications* 2021 12:1, 12(1), 1–8. <https://doi.org/10.1038/s41467-020-20314-w>
- 491 Moore, G. W. K., Schweiger, A., Zhang, J., & Steele, M. (2019). Spatiotemporal Variability of
 492 Sea Ice in the Arctic's Last Ice Area. *Geophysical Research Letters*, 46(20), 11237–11243.
 493 <https://doi.org/10.1029/2019GL083722>
- 494 Nghiem, S. V., Chao, Y., Neumann, G., Li, P., Perovich, D. K., Street, T., & Clemente-Colón, P.
 495 (2006). Depletion of perennial sea ice in the East Arctic Ocean. *Geophysical Research*
 496 *Letters*, 33(17). <https://doi.org/10.1029/2006GL027198>
- 497 Overland, J. E., & Wang, M. (2005). The Arctic climate paradox: The recent decrease of the
 498 Arctic Oscillation. *Geophysical Research Letters*, 32(6), L06701.
 499 <https://doi.org/10.1029/2004GL021752>
- 500 Overland, James E, & Wang, M. (2010). Large-scale atmospheric circulation changes are
 501 associated with the recent loss of Arctic sea ice. *Tellus A: Dynamic Meteorology and*

- 502 *Oceanography*, 62(1), 1–9. <https://doi.org/10.1111/J.1600-0870.2009.00421.X>
- 503 Peng, G., Meier, W. N., Scott, D. J., & Savoie, M. H. (2013). A long-term and reproducible
504 passive microwave sea ice concentration data record for climate studies and monitoring.
505 *Earth System Science Data*, 5(2), 311–318. <https://doi.org/10.5194/essd-5-311-2013>
- 506 Perovich, D. K., Light, B., Eicken, H., Jones, K. F., Runciman, K., & Nghiem, S. V. (2007).
507 Increasing solar heating of the Arctic Ocean and adjacent seas, 1979–2005: Attribution and
508 role in the ice-albedo feedback. *Geophysical Research Letters*, 34(19), L19505.
509 <https://doi.org/10.1029/2007GL031480>
- 510 Peterson, I., Hamilton, J., Prinsenber, S., & Pettipas, R. (2012). Wind-forcing of volume
511 transport through Lancaster Sound. *Journal of Geophysical Research: Oceans*, 117(C11).
512 <https://doi.org/10.1029/2012JC008140>
- 513 Peterson, I. K., Pettipas, R., & Rosing-Asvid, A. (2015). Trends and Variability in Sea Ice and
514 Icebergs off the Canadian East Coast. *Atmosphere-Ocean*, 53(5), 582–594.
515 <https://doi.org/10.1080/07055900.2015.1057684>
- 516 Polyakov, I. V., Alexeev, V. A., Bhatt, U. S., Polyakova, E. I., & Zhang, X. (2010). North
517 Atlantic warming: patterns of long-term trend and multidecadal variability. *Climate*
518 *Dynamics*, 34(2), 439–457. <https://doi.org/10.1007/s00382-008-0522-3>
- 519 Polyakov, I. V., Beszczynska, A., Carmack, E. C., Dmitrenko, I. A., Fahrback, E., Frolov, I. E.,
520 ... Walsh, J. E. (2005). One more step toward a warmer Arctic. *Geophysical Research*
521 *Letters*, 32(17). <https://doi.org/https://doi.org/10.1029/2005GL023740>
- 522 Ramos da Silva, R., & Avissar, R. (2005). The impacts of the Luni-Solar oscillation on the
523 Arctic oscillation. *Geophysical Research Letters*, 32(22), 1–4.
524 <https://doi.org/10.1029/2005GL023418>
- 525 Rigor, I. G., & Wallace, J. M. (2004). Variations in the age of Arctic sea-ice and summer sea-ice
526 extent. *Geophysical Research Letters*, 31(9). <https://doi.org/10.1029/2004GL019492>
- 527 Rigor, I. G., Wallace, J. M., Colony, R. L., Rigor, I. G., Wallace, J. M., & Colony, R. L. (2002).
528 Response of Sea Ice to the Arctic Oscillation. *Journal of Climate*, 15(18), 2648–2663.
529 [https://doi.org/10.1175/1520-0442\(2002\)015<2648:ROSITT>2.0.CO;2](https://doi.org/10.1175/1520-0442(2002)015<2648:ROSITT>2.0.CO;2)
- 530 Rimbu, N., Lohmann, G., Felis, T., & Pätzold, J. (2001). Arctic Oscillation signature in a Red
531 Sea coral. *Geophysical Research Letters*, 28(15), 2959–2962.
532 <https://doi.org/10.1029/2001GL013083>
- 533 Rimbu, N., Lohmann, G., Kim, J. H., Arz, H. W., & Schneider, R. (2003). Arctic/North Atlantic
534 Oscillation signature in Holocene sea surface temperature trends as obtained from alkenone
535 data. *Geophysical Research Letters*, 30(6), 1280. <https://doi.org/10.1029/2002GL016570>
- 536 Saenger, C., Cohen, A. L., Oppo, D. W., Halley, R. B., & Carilli, J. E. (2009). Surface-
537 temperature trends and variability in the low-latitude North Atlantic since 1552. *Nature*
538 *Geoscience*, 2(7), 492–495. <https://doi.org/10.1038/ngeo552>
- 539 Samelson, R. M., Agnew, T., Melling, H., & Münchow, A. (2006). Evidence for atmospheric
540 control of sea-ice motion through Nares Strait. *Geophysical Research Letters*, 33(2).
541 <https://doi.org/10.1029/2005GL025016>
- 542 Schlesinger, M. E., & Ramankutty, N. (1994). An oscillation in the global climate system of
543 period 65–70 years. *Nature* 1994 367:6465, 367(6465), 723–726.
544 <https://doi.org/10.1038/367723a0>
- 545 Shindell, D., & Faluvegi, G. (2009). Climate response to regional radiative forcing during the
546 twentieth century. *Nature Geoscience* 2009 2:4, 2(4), 294–300.
547 <https://doi.org/10.1038/ngeo473>

- 548 Sicre, M. A., Weckström, K., Seidenkrantz, M. S., Kuijpers, A., Benetti, M., Masse, G., ...
549 Mignot, J. (2014). Labrador current variability over the last 2000 years. *Earth and*
550 *Planetary Science Letters*, 400, 26–32. <https://doi.org/10.1016/J.EPSL.2014.05.016>
- 551 Stroeve, J. C., Maslanik, J., Serreze, M. C., Rigor, I., Meier, W., & Fowler, C. (2011). Sea ice
552 response to an extreme negative phase of the Arctic Oscillation during winter 2009/2010.
553 *Geophysical Research Letters*, 38(2), 2502. <https://doi.org/10.1029/2010GL045662>
- 554 Thompson, D. W. J., & Wallace, J. M. (1998). The Arctic oscillation signature in the wintertime
555 geopotential height and temperature fields. *Geophysical Research Letters*, 25(9), 1297–
556 1300. <https://doi.org/10.1029/98GL00950>
- 557 Trenberth, K. E., & Paolino, D. A. (1980). The Northern Hemisphere Sea-Level Pressure Data
558 Set: Trends, Errors and Discontinuities. *Monthly Weather Review*, 108(7), 855–872.
559 [https://doi.org/10.1175/1520-0493\(1980\)108<0855:TNHSLP>2.0.CO;2](https://doi.org/10.1175/1520-0493(1980)108<0855:TNHSLP>2.0.CO;2)
- 560 Trusel, L. D., Das, S. B., Osman, M. B., Evans, M. J., Smith, B. E., Fettweis, X., ... van den
561 Broeke, M. R. (2018). Nonlinear rise in Greenland runoff in response to post-industrial
562 Arctic warming. *Nature* 2018 564:7734, 564(7734), 104–108.
563 <https://doi.org/10.1038/s41586-018-0752-4>
- 564 Wallace, D. W. J., & Thompson, J. M. (2000). Annular Modes in the Extratropical Circulation.
565 Part I: Month-to-Month Variability. *Journal of Climate*, 13(5), 1000–1016.
566 [https://doi.org/10.1175/1520-0442\(2000\)013<1000:AMITEC>2.0.CO;2](https://doi.org/10.1175/1520-0442(2000)013<1000:AMITEC>2.0.CO;2)
- 567 Williams, S., Adey, W. H., Halfar, J., Kronz, A., Gagnon, P., Bélanger, D., & Nash, M. (2018).
568 Effects of light and temperature on Mg uptake, growth, and calcification in the proxy
569 climate archive *Clathromorphum compactum*. *Biogeosciences*, 15(19), 5745–5759.
- 570 Williams, Siobhan, Halfar, J., Zack, T., Hetzinger, S., Blicher, M., & Juul-Pedersen, T. (2019).
571 Reprint of Comparison of climate signals obtained from encrusting and free-living rhodolith
572 coralline algae. *Chemical Geology*, 526, 175–185.
573 <https://doi.org/10.1016/J.CHEMGEO.2018.02.030>
- 574 Williams, Siobhan, Halfar, J., Zack, T., Hetzinger, S., Blicher, M., Juul-pedersen, T., ... van de
575 Berf, W. J. (2018). Coralline Algae Archive Fjord Surface Water Temperatures in
576 Southwest Greenland. *Journal of Geophysical Research: Biogeosciences*, 123, 2617–2626.
577 <https://doi.org/10.1029/2018JG004385>
- 578 Willis, M. D., Leaitch, W. R., & Abbatt, J. P. D. (2018). Processes Controlling the Composition
579 and Abundance of Arctic Aerosol. *Reviews of Geophysics*, 56(4), 621–671.
580 <https://doi.org/10.1029/2018RG000602>
- 581 Yang, H., Wang, K., Dai, H., Wang, Y., & Li, Q. (2016). Wind effect on the Atlantic meridional
582 overturning circulation via sea ice and vertical diffusion. *Climate Dynamics*, 46(11), 3387–
583 3403. <https://doi.org/10.1007/s00382-015-2774-z>
- 584 Young, G. H. F., McCarroll, D., Loader, N. J., Gagen, M. H., Kirchhefer, A. J., & Demmler, J.
585 C. (2012). Changes in atmospheric circulation and the Arctic Oscillation preserved within a
586 millennial length reconstruction of summer cloud cover from northern Fennoscandia.
587 *Climate Dynamics*, 39(1–2), 495–507. [https://doi.org/10.1007/S00382-011-1246-](https://doi.org/10.1007/S00382-011-1246-3/FIGURES/5)
588 [3/FIGURES/5](https://doi.org/10.1007/S00382-011-1246-3/FIGURES/5)
- 589 Zhang, X., & Walsh, J. E. (2006). Toward a Seasonally Ice-Covered Arctic Ocean: Scenarios
590 from the IPCC AR4 Model Simulations. *Journal of Climate*, 19(9), 1730–1747.
591 <https://doi.org/10.1175/JCLI3767.1>
- 592